

TEAM2024-00017

OPTIMIZATION HYBRID PATH PLANNING BASED ON A-STAR ALGORITHM COMBINING WITH DWA

THAI-VIET DANG

¹School of Mechanical Engineering, Hanoi University of Science and Technology, Hanoi, Vietnam

*Corresponding author; e-mail: viet.dangthai@hust.edu.vn

Abstract

While dealing with dynamic scenarios, mobile robot (MR) path planning (PP) has proven to be extremely challenging. To overcome difficulties with grid-map representation, the paper proposes a hybrid path planning strategy. In a typical setting, an A-star algorithm first generates a global path planning (GPP). To ensure safe obstructive avoidance, the modified heuristic function is enhanced with a risk cost coefficient adjusted according to the distance to the nearest obstacle. Then, GPP is improved by eliminating redundant nodes, and smoothing algorithms. Furthermore, local path planning (LPP) has enhanced the ability to avoid obstacles in local areas by using adaptive dynamic window approach (DWA). The obtained path is hardly continuous after eliminating unnecessary path nodes and the required recalculation LPP based on DWA. Consequently, straight, and curved segments are joined into the continuous polyline smoothed by the Bezier curves. The proposed hybrid PP has been shown to be feasible and to produce optimal outcomes in both simulations and experiments.

Keywords:

A-star algorithm, Bezier curve, dynamic window approach (DWA), obstacle avoidance, hybrid path planning

1 INTRODUCTION

Simultaneous localization and mapping (SLAM) and motion planning represent two of the most pivotal challenges encountered by MRs [Maulana 2018]. Path planning (PP) is a term utilized within the field of robotics to describe the procedure of decomposing the intended movement task into distinct motions that adhere to movement constraints and potentially enhance a particular aspect of the motion [Patle 2019]. PP can be categorized broadly into two primary methodologies: GPP and LPP [Dang 2023a]. GPP devises an optimal route on a known global environment. Traditionally, techniques like Dijkstra [Alshammrei 2022], A-star [Dang 2023b], RRT-star [Dang 2023c], and D-star [Lin 2023] have served as the foundation of GPP. While the Dijkstra algorithm is uncomplicated in static environments, it tends to exhibit reduced efficiency and slower path optimization in larger, more dynamic settings [Alshammrei 2022]. The A-star algorithm, an advancement from Dijkstra, incorporates a heuristic function that facilitates rapid identification of the shortest path on grid maps [Dang 2023d]. Nevertheless, its planned trajectory might bring the mobile robots (MRs) into close proximity with obstacles, potentially endangering them with collisions. The dynamic D*Lite algorithm, a progression tailored for dynamic environments, tackles concerns related to efficiency and power consumption [Lin 2023]. Despite its efficacy in unfamiliar environments, D*Lite is burdened by certain

drawbacks, such as sluggish planning efficiency, numerous path nodes, and turning points in extensive environments. The local path planning algorithm represents a methodology designed for dynamic environments [Dang 2023e]. Conversely, LPP strategies excel in real-time obstacle evasion but lack the holistic supervision provided by GPP, often resulting in suboptimal path choices in the broader scope of the robot's mission. MRs frequently rely on approaches like the Artificial Potential Field (APF), DWA, and Time Elastic Band (TEB) to maneuver around obstacles [Liu 2021]. The APF is renowned for its high safety and smoothness levels during practical operations. Nevertheless, its effectiveness is confined to local search regions, especially when obstacles are positioned near the target, potentially hindering MRs from reaching their designated destination [Li 2024]. The DWA, serving as a method to sample information from the ever-changing local surroundings, enables MRs to anticipate the subsequent motion state based on their current state. In comparison to APF, DWA accomplishes swifter planning, guarantees safety and dependability, and upholds robust real-time performance [Yang 2022]. Nevertheless, while DWA adeptly evades both stationary and moving obstacles, its dependency on global environmental elements stands out as a notable constraint. This paper proposes an optimal HPP algorithm for MRs. A novel heuristic function is integrated with coefficients linked to distance and direction

to streamline search time and diminish the number of steps when constructing GPP based on A-star. Furthermore, DWA bolsters the velocity and acceleration of MRs in response to local dynamic environmental alterations in accordance with the GPP direction. To summarize, the proposed methodology refines GPP data to navigate around dynamic obstacles, thereby amplifying real-time performance and flexibility.

2 GPP BASED ON IMPROVED A-STAR

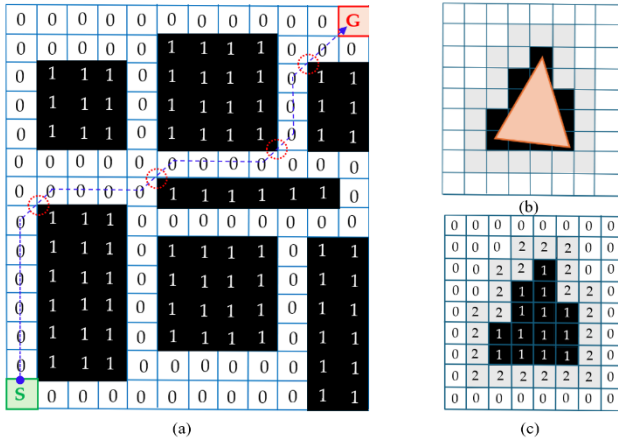


Fig. 1: MR's grid map-based environment with (a): a grid map, (b): a obstacles having risk surrounding and (c): the values of different cells in grid map.

The MR's environment is modelled by the grid-map method that obstacle cell has value of 1, movement cell has value of 0, and the risk surrounding obstacle has value of 2, in Fig. 1. Based on A-star heuristic function [Dang 2023f], a new grid map is reconstructed to ensure safe obstructive avoidance (see Fig. 1c) with a risk cost coefficient adjusted according to the distance to the nearest obstacle (see Fig. 1b). Then, (1) selects the nodes being the closest distance from the start node S to the goal node G (blue dashed line).

$$f(n) = g(n) + h(n) + r(n), \quad (1)$$

where n : the current node; $g(n)$: the actual cost from n to the following node; $h(n)$: the predicted cost from n to goal (G); $f(n)$: the total cost evaluation; and $r(n)$: the risk cost depending on the distance to obstacle.

Because only the distance without the direction is considered in Eq. (1), which leads to the difficulty of trajectory optimization, reduces the search efficacy in larger environment. In complex scenarios, the robot will fall into loops and traps and cannot react to moving obstacles. A modified $h(n)$ in Eq. (2) aims to solve the existing problems in (1) and support the provision of additional information to DWA when applied to LPP.

$$f(n) = g(n) + (aL + b \cos \theta)h(n) + r(n), \quad (2)$$

where the current MR's position L is defined as follows:

$$L = dx + dy - (2 - \sqrt{2}) \min(dx, dy), \quad (3)$$

and θ is the angle of the first direction from the parent node to the expanded node and the second direction from the expanded node to the targeted node. The value of $\cos \theta$ is changed from -1 to +1 to MR always reach to the target node while avoiding the obstacles. Therefore, the search efficiency is improved with the optimal time processing. One of the disadvantages of the A-star algorithm is that the number of node points in the search algorithm is too redundant.

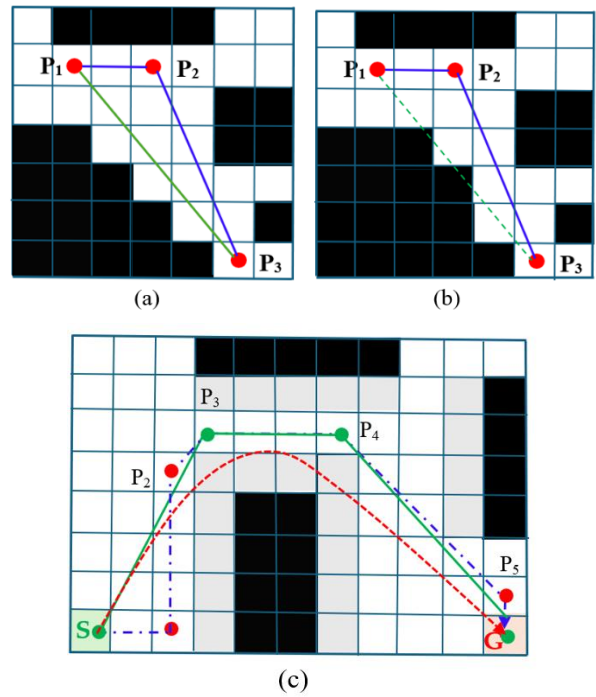


Fig. 2. The JPS with (a): successful JPS; (b): unsuccessful JPS; and (c): applied JPS in GPP (red dashed line).

When the robot finds a path and avoids it in a dynamic local environment, the calculation process will be repeated, causing the number of calculation steps to increase, directly affecting the robot control process when following the navigation plan, causing delays. During the calculation and data transmission process, it also causes errors that affect the quality of the control process. The proposed algorithm introduces the JPS technique to eliminate redundant points (see Figs. 2a and 2b), combined with the improved Bezier curves to connect straight and curved segments into the continuous smooth trajectory in following Eq. (4):

$$B_5(t) = \sum_{k=0}^5 \binom{5}{k} (1-s)^{5-k} s^k b_k, \quad 0 \leq s \leq 1, \quad (4)$$

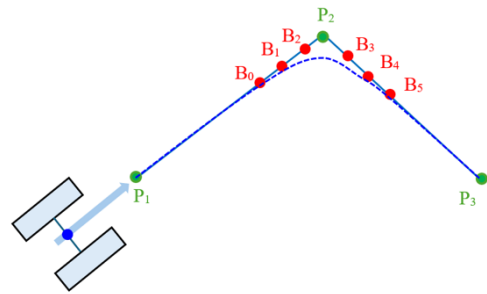


Fig. 3. The fifth order Bezier curve (blue dot line) for three path points of P_1 , P_2 , and P_3 using 6 Bezier points of (B_0, B_2, B_5) .

One distinguishing feature of a Bezier curve is that the tangents at the endpoint are entirely dictated by the adjacent control points. Fig. 3 illustrates the fifth order Bezier curve with six control points of (B_0, B_1, \dots, B_5) in which (B_0, B_1, B_2) and (B_3, B_4, B_5) are collinear, respectively. By utilizing parameterization of the control points within the Bezier curves, the MR's trajectory is able to effectively follow prescribed path points P_i while adhering to specified kinematic constraints.

Finally, the trajectory optimization aims to minimize path length, reduce steering angle variations, and minimize overall cost. Additionally, a smoothed GPP is generated through the seamless connection of linear path segments and Bezier curves in Figs. 2c.

3 LPP BASED ON ADAPTIVE DWA

Firstly, MR's kinematics model each Δt is illustrated in following Eq. (5):

$$\begin{cases} x(t+1) = x(t) + v_t \Delta t \cos \theta_t \\ y(t+1) = y(t) + v_t \Delta t \sin \theta_t, \\ \theta(t+1) = \theta(t) + \omega_t \Delta t \end{cases} \quad (5)$$

Throughout the optimization process of the objective function delineated in optimal GPP, the MR's dynamic window is modified in an adaptive manner based on speed constraints, acceleration constraints, and the necessity to avoid obstacles. LPP uses GPP points for local target points. Hence, the respective sampling spaces can be characterized as follows:

$$\begin{aligned} v_s &= \left\{ (v, \omega) \mid |v| \leq v_{\max} \cap |\omega| \leq \omega_{\max} \right\}, \\ v_d &= \left\{ (v, \omega) \mid v \in [v_0 - a_{\max} \Delta t, v_0 + a_{\max} \Delta t] \right. \\ &\quad \left. \cap [\omega_0 - \alpha_{\max} \Delta t, \omega_0 + \alpha_{\max} \Delta t] \right\}, \\ v_a &= \left\{ (v, \omega) \mid |v| \leq \sqrt{2 \text{dist}(v, \omega) a_{\max}} \right\}, \end{aligned} \quad (6)$$

where v_0 , and ω_0 : the MR's initial values of v and ω , respectively. v_{\max} , ω_{\max} , a_{\max} , and α_{\max} stand for the peak values of the MR's speed, angular speed, linear acceleration, and angular acceleration, respectively. Δt indicates the time interval between samples. The above given restrictions imposed on the DWA for the velocities v_r based on the speed space v_s , in Fig. 4. Then the area v_r is defined as the intersection of (v_s, v_a, v_d) in Eq. (7)

$$v_r = v_s \cap v_a \cap v_d \quad (7)$$

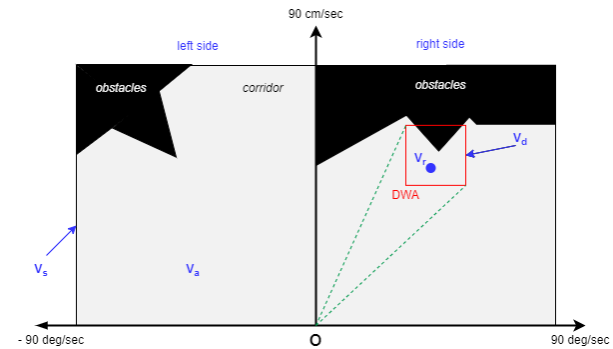


Fig. 4. The representation of MR's speed space.

While all conditions in Eq. (6) are satisfied, it is crucial to enhance the optimization of the DWA's evaluation function to effectively discover the optimal LPP. Eq. (8) presents the formulation of the adaptive DWA's evaluation function for MR.

$$F(v, \omega) = \sigma \{ \alpha * \text{head}(v, \omega) + \beta * \text{dist}(v, \omega) + \gamma * \text{vel}(v, \omega) \}, \quad (8)$$

where $\text{head}(v, \omega)$: the azimuthal deviation effectively ensuring the MR follows the locally optimal path; $\text{dist}(v, \omega)$: the distance between the MR's predicted path end and the nearest obstacle. $\text{vel}(v, \omega)$: the velocity of the current simulated trajectory; ω : the filtering coefficient; α , β , and γ : the weighting coefficients. Fig. 5 presents an azimuth

assessment into the evaluation process ensures the fulfillment of various objectives including identifying the shortest route, navigating dynamic obstacles, and maintaining smoothness.

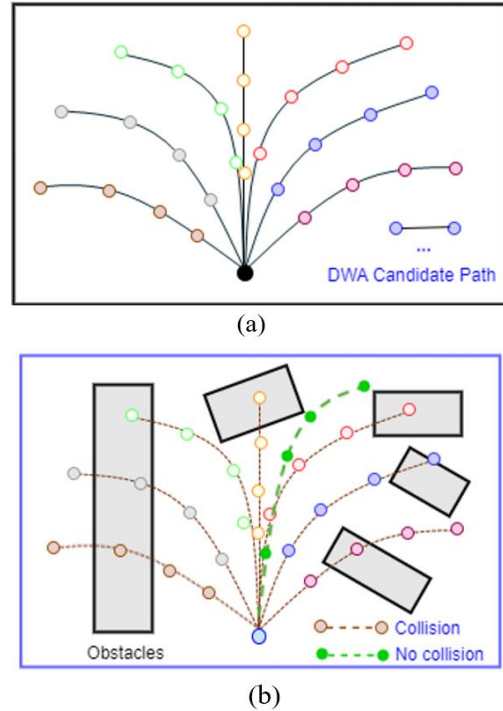


Fig. 5. The adaptive DWA's evaluation function with (a): DWA candidate path and (b) Optimal DWA path.

In summary, GPP cannot handle dynamic obstacles changing their position. Therefore, LPP based on DWA deals with dynamic obstacles. The optimal strategy of hybrid path planning is illustrated in Fig. 6.

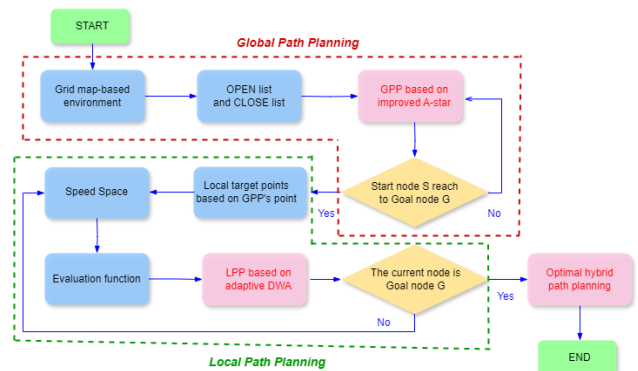


Fig. 6. The optimal strategy of hybrid path planning (HPP).

4 RESULTS AND DISCUSSION

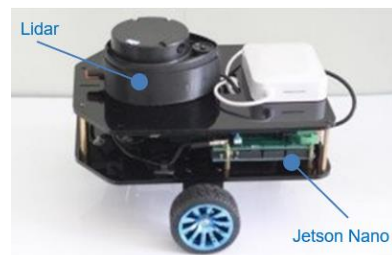


Fig. 7. The three wheeled MR equipped Lidar and Jetson Nano.

On a cutting-edge computer boasting 32 GB of Ram, powered by an Intel Core i7-11400H processor, with a VGA

GeForce RTX 3060, and running Windows 11, a vast 50x50 grid map was meticulously crafted, with the starting point marked as S (0, 0). Employing a three-wheeled mobile robot (see Fig. 7), the forthcoming experiment is conducted to validate the viability of the suggested PP.

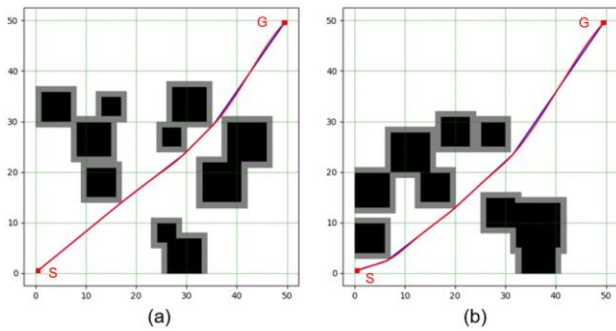


Fig. 8. The improved GPP using JPS and Bezier in simple environments with A-star path (blue line) and improved A-star path (red line).

In scenario 1, the number of static obstacles is concentrated in the lower left corner, the space between the obstacles is large. Therefore, the improved A-star algorithm can easily build a feasible navigation plan connecting the starting point S to the destination point G. However, JPS and smoothed technique have also been effective in smoothing the improved A-star path. path. path. This result will also help the MR move stably, the turning angle changes little and follow the guidance GPP.

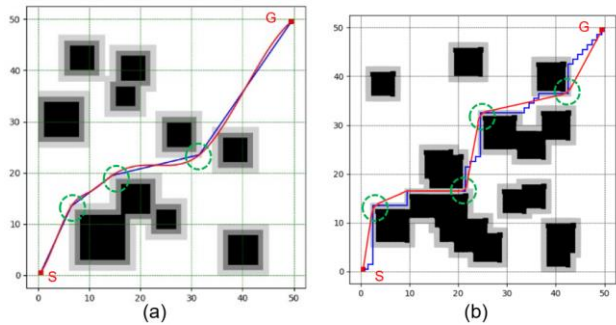


Fig. 9. The improved GPP using JPS and Bezier in complex environments with A-star path (blue line) and improved A-star path (red line).

Scenario 2 increases the difficulty with the number of static obstacles and density distributed in the environment. In Figure 9a, using the enhanced heuristic function, the A-star algorithm can establish navigation to avoid obstacles with different levels of safe distance (gray zone). Incorporating a fifth degree Bezier line makes GPP smoother, meaning the change in angular direction when MR tracking trajectory also changes little. In particular, MR still ensures the ability to avoid collisions with the corners of obstacles while still maintaining the direction of movement (green dashed line circle). As the environment becomes more complex in Fig. 9b, we can easily see that the A-star control path points become more numerous, which affects the search speed of the algorithm. Besides also increasing the travel distance, the application of JPS and smoothed technique helps to dramatically reduce P_i control path points. Furthermore, the Bezier curve also supports the process of smoothing the obtained GPP curve.

In Fig. 10, the MR executes the optimal strategy of HPP in accordance with a secure LPP combining with the adaptive DWA. The depiction in Fig. 10a illustrates the MR's local path, which facilitates evasion of both stationary and

dynamic obstacles 1 and 2. The MR, guided by the innovative hybrid path planning approach, detects the initial static obstacle as depicted in Fig. 10b and successfully navigates around it following the prescribed GPP. Subsequently, upon executing a turn, the MR leverages the DWA method to compute the distance from the diagonally advancing obstacle 1, thereby evading it effectively. The efficacy of the proposed hybrid path planning becomes evident when dynamic obstacle 1 maneuvers, causing a constriction in the available space for movement. This successful negotiation of a narrow passage to the target destination by the robot in Figs. 10c and 10d underscores the effectiveness of the hybrid path planning method.

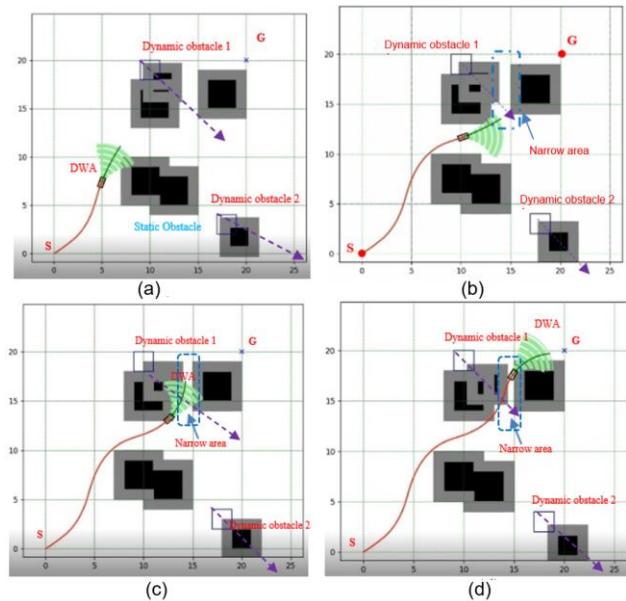


Fig. 10. MR's Optimal HPP using adaptive DWA in local areas with (a): turning around the static obstacle corner, (b): adjusting the MR's speed when discovering dynamic obstacle, (c): avoiding a dynamic obstacle and turn to move through the narrow area, and (d): moving through successfully the narrow area.

However, LPP using adaptive DWA will need to recalculate in each local region leading to increased computation. In practical control, stable and accurate control process is always required, so our proposed optimal hybrid path planning will require appropriate data processing and calculation systems and is also a development direction for integrating MR's perception system with optimized training resources and processing speed.

5 CONCLUSIONS

The paper proposed the optimal strategy of hybrid path planning, combining strategies to optimize various tasks such as dynamic obstacle avoidance and trajectory smoothness. Using the A-star algorithm as a foundation, unnecessary nodes in the GPP are eliminated by applying JPS. Whether faced with stationary or moving obstacles, MRs navigates with cobstaclesizing customizable danger zones around the obstacles. Additionally using fifth degree Bezier curves, MR's path is continuously refined to ensure a steady and secure movement. Hence, after completing LPP, optimal HPP is created a smoothed GPP connecting linear control path segments and curves. Ultimately, this innovative technique effectively tackles the complexities of dynamic obstacles through enhancements in the adaptive DWA during LPP.

6 ACKNOWLEDGMENTS

Lab-506: Computer Vision and Autonomous Mobile Robot (CVAMS), VJIIST, HUST is gratefully acknowledged for providing work location, guidance, and expertise.

7 REFERENCES

- [Alshammrei 2022] Alshammrei, S. et al. Improved Dijkstra Algorithm for Mobile Robot Path Planning and Obstacle Avoidance. *Computers, Materials & Continua*, 2022, Vol.72, No.3, pp 5939-5954.
- [Dang 2023a] Dang, T.V. and Bui, N.T. Multi-Scale Fully Convolutional Network-Based Semantic Segmentation for Mobile Robot Navigation. *Electronics*, 2023, Vol.12, No.3, pp 533.
- [Dang 2023b] Dang, T.V., Nguyen, D.S. Optimal Navigation Based on Improved A* Algorithm for Mobile Robot. *Intelligent Systems and Networks*, 2023, LNNS, Vol.752, pp 574-580.
- [Dang 2023c] Dang, T.V. Research and design of a path planning using an improved RRT * algorithm for an autonomous mobile robot. *MM Science Journal*, 2023, Vol.10, pp 6712-6716.
- [Dang 2023d] Dang, T.V. Autonomous mobile robot path planning based on enhanced A* algorithm integrating with time elastic band. *MM Science Journal*, 2023, Vol. 10, pp 6717-6722.
- [Dang 2023e] Dang, T.V., Tran, D.M.C., and Tan, P.X. IRDC-Net: Lightweight Semantic Segmentation Network Based on Monocular Camera for Mobile Robot Navigation. *Sensors*, 2023, Vol.23, No.15, pp 6907.
- [Dang 2023f] Dang, T.V. and Bui, N.T. Obstacle Avoidance Strategy for Mobile Robot Based on Monocular Camera. *Electronics*, 2023, Vol.12, No.8., pp 1932.
- [Li 2024] Li, X., Li, G., Bian, Z. Research on Autonomous Vehicle Path Planning Algorithm Based on Improved RRT* Algorithm and Artificial Potential Field Method. *Sensors*, 2024, Vol.24, No.12, pp 3899.
- [Lin 2023] Lin, Z., Lu, L., Yuan, Y., & Zhao, H. A Novel Robotic Path Planning Method in Grid Map Context Based on D* Lite Algorithm and Deep Learning. *Journal of Circuits, Systems, and Computers*, 2023, Vol.33, No.4, pp 2450057
- [Liu 2021] Liu, L. et al. Global Dynamic Path Planning Fusion Algorithm Combining Jump-A* Algorithm and Dynamic Window Approach. *IEEE Access*, 2021, Vol.9, pp 19632-19638.
- [Maulana 2018] Maulana, I., Rasdina, A., and Priramadhi, R.A. Lidar Application for Mapping and Robot Navigation on Closed Environment. *Journal of Measurements Electronics Communications and Systems*, 2018, Vol.4, No.1, pp 767-782.
- [Patle 2019] Patle, B.K., Pandey, A., Parhi, D.R., and Jagadees, A. A review: on path planning strategies for navigation of mobile robot. *Defence Technology*, 2019, Vol.15, No.4, pp 582-606.
- [Yang 2022] Yang, H., and Teng, X. Mobile Robot Path Planning Based on Enhanced Dynamic Window Approach and Improved A* Algorithm. *Journal of Robotics*, 2022, Vol.2022, No.2, pp 1-9.